Fracture Mechanics of Concrete Structures
Proceedings FRAMCOS-3
AEDIFICATIO Publishers, D-79104 Freiburg, Germany

MICROFRACTURAL PULLOUT MODEL OF STEEL FIBER REINFORCED CONCRETE

S. Sumitro
Japan Structural Engineering and Computer Corporation, Tokyo, Japan
T. Tsubaki
Dept. of Civil Engineering, Yokohama National University, Yokohama, Japan

Abstract
It is considered important from an engineering point of view to investigate the toughening mechanism of steel fiber reinforced concrete (SFRC) which is a widely used construction material with improved mechanical properties. The tension pullout of a steel fiber from concrete matrix is recognized as one of the basic tests to obtain the deformational mechanical behavior of SFRC. Based on the pullout test of steel fibers with various embedding conditions, in this study, a pullout model that can describe the microfractural behavior of SFRC is presented. The mechanical behavior of steel fiber in concrete matrix in the present model is characterized by an interface zone referred to shear lag between the rigid concrete matrix and the steel fiber. The fiber-matrix debonding is considered by the fracture mechanical approach where the criterion for propagation of the debonded fiber-matrix interface is expressed in terms of the energy equilibrium. The parameters involved in the present model are the shear stiffness of the fiber-matrix boundary layer, the effective elastic modulus after debonding and the work of fracture of the debonded zone. Those parameters are determined from experimental data. The tensile rupture of the fiber, the effect of the end condition of fiber and the effect of the fiber geometry are also taken into account. The validity of the model is confirmed by the comparison with experimental results.
Key words: steel fiber reinforced concrete, microfracture, pullout model, energy criterion

1 Introduction

The mechanical behavior of brittle composite materials such as concrete can be improved by the inclusion of high-strength steel fibers with small-diameter (see Li, et al.(1991)). In order to make SFRC used as a structural material, it is essential to understand the microscopic deformational behavior and reinforcing mechanism of the steel fiber in concrete matrix (see, e.g., Naaman and Shah (1976), and Sumitro and Tsubaki (1996)). The bond between the fiber and the matrix is an important factor to be considered when dealing with modeling of the microscopic mechanical behavior of SFRC (see Ouyang and Shah (1994)). The basic test to obtain the fiber-matrix bond parameters is the fiber pullout test that significantly depends on the fiber geometry (see Tsubaki, et al.(1997, 1998)). Therefore, in this study, a microfractural fiber pullout model is proposed to characterized various fiber debonding and pullout properties. The validity and appropriateness of the model is verified by the comparison with the experimental data.

2 Modeling of fiber pullout

2.1 Theoretical background

A single fiber of a length of L is embedded in a matrix. The concrete matrix is assumed to be rigid except for a thin interface layer idealized as an interface with shear stiffness, k. Various types of fiber geometry are used in practice. Basically it can be categorized as three kinds of fiber shape, i.e., straight fiber, hooked fiber and anchored fiber. In this study, the end effect of fiber is modeled by a spring with a spring constant, k_{end}. As an example for schematic description, Fig. 1 shows the modeling of a single hooked type steel fiber which is bridging at a crack surface.

The fiber is assumed to have a constant cross-sectional area, A_f, and an initial elastic modulus, E_{f0}. The effect of Poisson's ratio is neglected for both fiber and matrix. It is assumed that debonding has occurred over a length, a, starting at $x=L$. Assuming that a constant shear stress is acting along the debonded interface layer, it can be written that (Ouyang and Shah (1994))

$$q = kU(x), \qquad 0 \le x \le L - a \tag{1}$$

$$q = q_f, \qquad L - a < x < L \tag{2}$$

where q is the shear force per unit length acting on the fiber. q_f is the frictional shear force per unit length, and $U(x)$ is the fiber displacement.

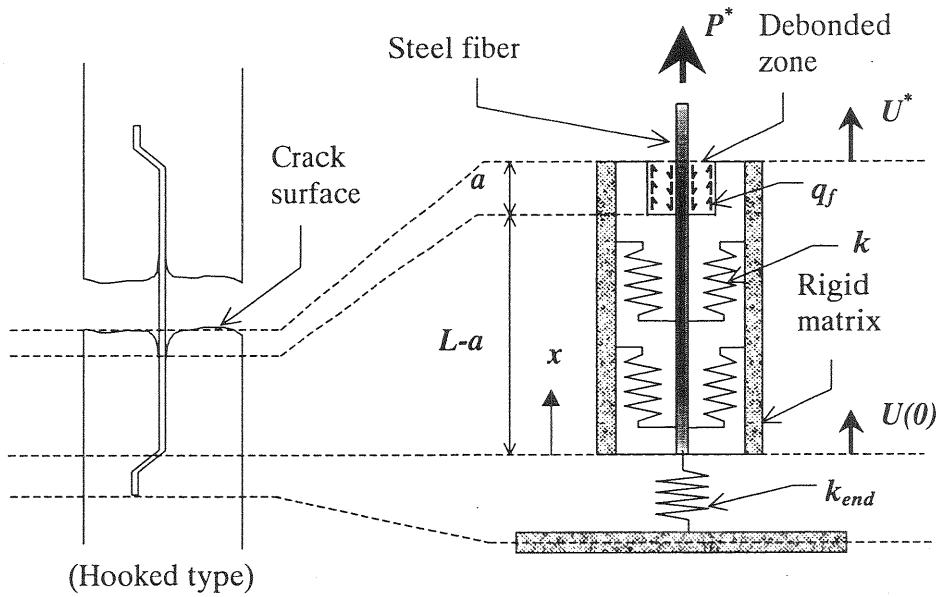

Fig. 1. Single fiber model at crack surface

Denoting the fiber force by P, the equilibrium equation is expressed as

$$P_{,x} - q = 0 \tag{3}$$

where a comma preceding a subscript indicates a differential operator, i.e., $(\ )_{,x}$ is the derivative with respect to x. Introducing the constitutive relationship for the fiber, the following equation is obtained.

$$P = E_f A_f U_{,x} \tag{4}$$

Then, the following differential equations for U are obtained:

$$U_{,xx} - \omega^2 U = 0, \qquad 0 \le x \le L - a \tag{5}$$

$$U_{,xx} - q_f / (E_f A_f) = 0, \quad L - a < x < L \tag{6}$$

with the quantity ω defined by $\omega = \sqrt{k/(E_f A_f)}$.

Introducing P^* as the pullout force at x=L, the boundary conditions are prescribed as

$$k_{end} U(0) = P(0) \tag{7}$$

$$E_f A_f U_{,x}(L) = P^* \tag{8}$$

The continuity conditions in displacement and fiber load at $x=L-a$ require

$$U(L-a)^{-} = U(L-a)^{+} \tag{9}$$

$$U_{,x}(L-a)^{-} = U_{,x}(L-a)^{+} \tag{10}$$

Solving the above set of equations, the following solutions for the fiber displacement are obtained:

$$U(x) = \frac{P^{*} - q_f a}{E_f A_f \omega}\left\{\frac{\cosh(\omega x)}{\alpha_1} + \frac{\sinh(\omega x)}{\alpha_2}\right\}, \qquad 0 \le x \le L-a \tag{11}$$

$$\begin{aligned} U(x) = {} & \frac{P^{*} - q_f a}{E_f A_f \omega}\left\{\frac{\cosh[\omega(L-a)]}{\alpha_1} + \frac{\sinh[\omega(L-a)]}{\alpha_2}\right\} \\ & - \frac{q_f}{2E_f A_f}(L-a)^2 - \frac{P^{*} - q_f L}{E_f A_f}(L-a) \\ & + \frac{q_f}{2E_f A_f}x^2 + \frac{P^{*} - q_f L}{E_f A_f}x, \qquad L-a < x \le L \end{aligned} \tag{12}$$

where

$$\alpha_1 = \frac{k_{end}}{E_f A_f \omega}\cosh[\omega(L-a)] + \sinh[\omega(L-a)] \tag{13a}$$

$$\alpha_2 = \frac{E_f A_f \omega}{k_{end}}\sinh[\omega(L-a)] + \cosh[\omega(L-a)] \tag{13b}$$

The displacement at the fiber end U^{*} is obtained from Eq.(12) as

$$U^{*} = \frac{P^{*} - q_f a}{E_f A_f \omega}\left\{\frac{\cosh[\omega(L-a)]}{\alpha_1} + \frac{\sinh[\omega(L-a)]}{\alpha_2}\right\} + \frac{P^{*} - \frac{1}{2}q_f a}{E_f A_f}a \tag{14}$$

2.2 Elastic Modulus

During a debonding propagation process, the surface layer of a fiber is considered to suffer local yielding due to stress concentration while being pulled out and cause the reduction of the elastic modulus of the fiber. The effective elastic modulus of the fiber, E_f, is modeled as:

$$E_f = E_{f0}, \qquad a = 0 \tag{15}$$

$$E_f = a_e E_{f0}, \qquad 0 < a \le L \tag{16}$$

where a_e is the effective modulus factor.

3 Criterion of fiber pullout

3.1 Fracture energy approach

The fracture criterion of the fiber-matrix interface is characterized by the basic assumption that debonding takes place when the energy release rate reaches a critical value that is related to the work of fracture of the interface, Γ. The propagation of the debonding zone requires a certain energy and this energy is characterized for the bond between the fiber and the matrix. The available energy for the crack growth is calculated from the elastic strain energy, Ωs, and the work done by the friction, Ω_f, at a certain load-deformation state of the system. For the purpose of simplicity, the strain energy is divided into three parts, i.e., the strain energy in the debonded part of the fiber, Ωs_1, the strain energy in the debonded part of the shear lag, Ωs_2, and the strain energy in the whole system for $x<L-a$, Ωs_3 (see Gao, et al. (1988)).

Knowing the fiber load and the constitutive equation for the fiber as expressed by Eq. 4, the strain energy in the debonded part of the fiber can be calculated as follows.

$$\Omega s_1 = \frac{1}{2E_f A_f}\int_{L-a}^{L}\left[P^* - q_f(L-x)\right]^2 dx = \frac{3P^* a(P^* - q_f a) + q_f^2 a^3}{6E_f A_f} \tag{17}$$

Assuring the displacement continuity at $x=L-a$, the strain energy in the debonded part of the fiber-matrix interface can be approximated as

$$\Omega s_2 = \frac{q_f a\left(\frac{P^*}{q_f} - 1\right)}{2E_f A_f \omega}\left\{\frac{\cosh\left[\omega(L-a)\right]}{\alpha_1} + \frac{\sinh\left[\omega(L-a)\right]}{\alpha_2}\right\} \tag{18}$$

Considering the fiber load at $x=L-a$, the strain energy in the whole system can be calculated and expressed as follows.

$$\Omega s_3 = \frac{(P^* - q_f)}{2E_f A_f \omega}\left\{\frac{\cosh\left[\omega(L-a)\right]}{\alpha_1} + \frac{\sinh\left[\omega(L-a)\right]}{\alpha_2}\right\} \tag{19}$$

Assuming that the displacement of matrix along the debonded interface are constant and given by $U(L-a)$, the work done by friction can be approximated as follows.

$$\Omega_f = \int_{L-a}^{L} q_f\left[U(x) - U(L-a)\right]dx = \frac{q_f\left\{-2q_f a^3 + 3P^* a^2\right\}}{6E_f A_f} \tag{20}$$

For a crack propagation from the debonded length a to $a+da$, the pullout load and the displacement at the pullout load changes by dP^* and dU^*. The energy release rate G in this transition can be written as

$$G = P^*\frac{dU^*}{da} - \frac{d\Omega s_1}{da} - \frac{d\Omega s_2}{da} - \frac{d\Omega s_3}{da} - \frac{d\Omega_f}{da} \tag{21}$$

Considering the condition when the debonding takes place, $G=\rho\Gamma$, where ρ is the perimeter of the fiber, the pullout load can be obtained and written as

$$P^* = \beta\left[\frac{q_f}{2\omega} + \sqrt{\left(\frac{q_f}{2\omega}\right)^2 + 2E_f A_f \rho\Gamma}\right] + q_f a \tag{22}$$

where

$$\beta = \frac{\alpha_1\alpha_2}{\alpha_1 \sinh[\omega(L-a)] + \alpha_2 \cosh[\omega(L-a)]} \tag{23}$$

3.2 Calculation algorithm

The pullout load-displacement (P^*-U) relationship can be expressed as follows. From the origin point the fiber has an elastic relationship which is referred to as elastic state. Once the required fracture energy is consumed, debonding process starts and propagates up to full debonding that occurs at the peak pullout load. The present model enables to control the tensile rupture of the fiber by comparing the tensile stress and the tensile strength of the fiber. This state is referred to as debonding state.

Right after reaching the peak load, a sudden failure occurs and the sustainable load drops to a certain level and the pullout process continues until the tensile rupture occurs at a reduced pullout load or until the fiber is totally pulled out. This state is referred to as pullout state.

The calculation algorithm of the pullout load-displacement relationship can be summarized as follows.

1. Evaluate the initial elastic modulus, fiber end spring constant and other related material parameter.
2. Calculate the displacement U (Eq.11) and the pullout load P^* (Eq.22) at the transition point from elastic state to debonding state with a=0.
3. Proceed to new load steps along debonding state with crack propagation $a^N=a^P+\Delta a$, where superscript P denotes the previous value while superscript N denotes the new value. Assume the displacement in the matrix shear lag along the debonded interface equals to $U(L\text{-}a^P)$, so that the shear force per unit length can be calculated as $q_f=kU(L\text{-}a^P)$. Calculate the current displacement U (Eqs.11,12) and the current pullout load P^* (Eq.22). Examine the tensile stress of the fiber at each load step.
4. Repeat step 3 until the tensile rupture occurs (i.e., when the tensile stress greater or equal to tensile strength), otherwise until full debonding occurs at a=L.

5. A sudden failure phenomenon is assumed to follow with the full debonding occurrence. Then, the remaining embedded part of fiber is assumed to provide a frictional resistance and the pullout force becomes $P^* = q_f(L-U_a)(a_fL-U)/(a_fL-U_a)$ where a_f is the effective frictional length factor to express the reduction of fiber length with frictional shear stress and U_a is the displacement at full debonding.
6. Repeat step 5 with imposed displacement until the tensile rupture occurs at $P^*=0$ or until the fiber is totally pulled out at $U = a_fL$.

4 Comparison with experimental results

4.1 Outline of experiment

A series of experiments were done to investigate the effect of fiber geometry on the mechanical properties of SFRC. The experiment is conducted by pulling out 32 fibers simultaneously. For the purpose of data fitting, the mean value of 32 fibers is assumed to represent the average deformational behavior of one fiber (see Tsubaki, et al (1997)). Three types of steel fibers were used, i.e., straight cut wire with indented surface, hooked cut wire with smooth surface and anchored stainless steel wire with a round block at both ends (see Fig. 2). The length of these fibers is 30 mm. The straight and hooked fibers have an equivalent diameter of 0.60 mm, an aspect ratio of 50 and tensile strength equal to or larger than 1000 N/mm^2. The anchored fiber has an equivalent diameter of 0.50 mm, an aspect ratio of 60 and mean tensile strength of 1000 N/mm^2.

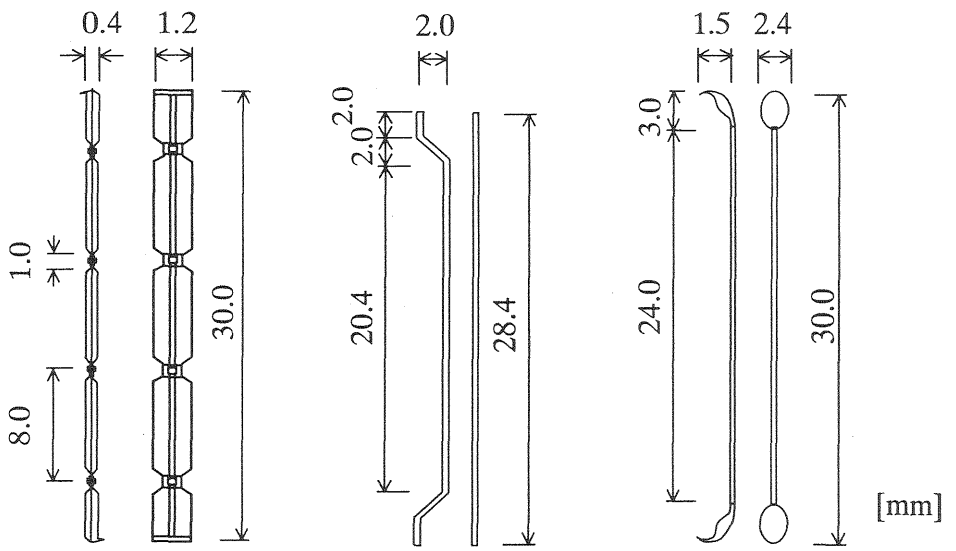

Fig.2. Steel fiber geometry

4.2 Determination of material parameters

To simulate the experimental results, the initial elastic modulus of steel fiber and the length of steel fiber are taken as E_{fo} = 2.0 x 10^5 N/mm^2 and L= 15 mm, respectively. By the analysis of test data on the average behavior of 32 fibers through the trial and error technique the optimum values of other material parameters are obtained as listed in Table 1. The data fits are shown in Fig. 3.

Table 1. Optimum values of material parameters

Fiber Geometry	d (mm)	k_{end} (N/mm)	Γ (N.m/m^2)	a_e	a_f
Straight type	0.60	0.0	1.7	0.027	0.60
Hooked type	0.60	2.0 x 10^4	2.1	0.018	0.45
Anchored type	0.50	4.0 x 10^4	1.8	0.063	0.15

Notes:
d : diameter of the fiber
k_{end} : spring constant at the end of the fiber
Γ : work of the fracture of the interface
a_e : effective modulus factor of the fiber
a_f : effective frictional length factor

The pullout force-displacement relationship for straight steel fiber starts from the elastic state, followed by the debonding state until the maximum pullout force. A sudden failure occurs at the peak, followed by a frictional fiber pull out state. The pullout force-displacement relationship of hooked steel fiber is expressed as follows. The full debonding phenomenon occurs around the maximum pullout force, followed by a sudden failure and simultaneous plastic deformation of the fiber hook. In these two geometrical shapes of steel fiber, no fiber rupture were observed in the experiment.

The deformational behavior for anchored steel fiber is expressed as follows. It is obtained from the average behavior of 32 anchored fibers that, after reaching the maximum pullout force, sudden failure occurs, followed by a small plastic deformation of the fiber, and in a small fiber pullout displacement, fiber rupture occurs. Furthermore, for a particular single fiber, the tensile rupture may occur before the average maximum pullout force. This phenomenon can also be simulated by applying the present model, in which, its tensile stress is checked at each load step.

The sharp drop of the pullout force at the peak observed in the simulation result may disappear in the case where the statistical variation of the material properties are considered. By the comparison with experimental results, it is confirmed that the numerical simulation using the present microfractural model can express the deformational behavior of SFRC with various fiber geometry satisfactorily.

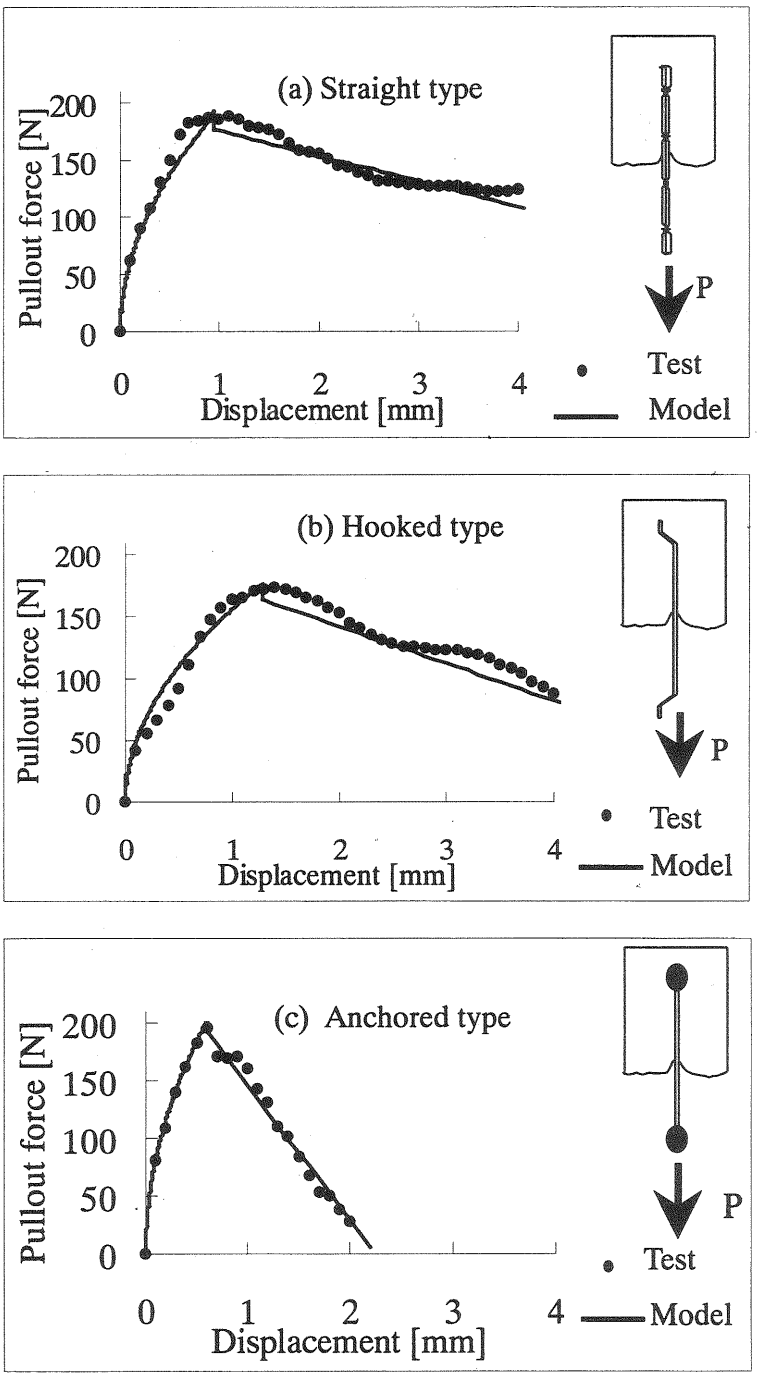

Fig. 3. Comparison between microfractural model and test data

5 Conclusion

A microfractural fiber pullout model is proposed for SFRC using the energy criterion for debonding. By the comparison with experimental results, it is confirmed that the present model is suitable to express the pullout behavior of SFRC with various fiber geometry under uniaxial tension. Various stages of the fiber pullout process are described by the present model.

6. References

Gao, Y.C., May, Y.W. and Cotterell, B. (1988) Fracture of fiber reinforced materials. **J. Applied Mathematics and Physics (ZAMP),** Vol. 39, 550-572.

Li, V.C., Wang, Y. and Backer, S. (1991) A micromechanical model of tension-softening and bridging toughening of short random fiber reinforced brittle matrix composites. **J. Mech. Phys. Solids,** Vol. 39, No. 5, 607-625.

Naaman, A.E. and Shah, S.P. (1976) Pull-out mechanism in steel fiber-reinforced concrete. **J. of Struct. Div., Proc. of ASCE**, Vol. 102, No. ST8, 1537-1548.

Ouyang, C. and Shah, S.P. (1994) Fracture energy apporach for predicting cracking of reinforced concrete tensile members. **ACI Structural Journal,** Vol. 91, No. 1, 69-78.

Sumitro, S. and Tsubaki, T. (1996) Micromechanical constitutive relationship of steel fiber reinforced concrete. **Transaction of the JCI**, Vol. 18, 159-166

Tsubaki, T., Sumitro, S. and Shoji, H. (1997) Modeling of tensile and shear mechanical properties of steel fiber reinforced concrte, **Concrete Research and Technology,** Vol. 8, No. 1, 233-241

Tsubaki, T. and Sumitro, S. (1998) Effect of fiber type on the mechanical behavior of steel fiber reinforced concrete subjected to uniaxial tension, **Proc. of EASEC-6 Conference, Taipei,** Vol. 3, 1959-1964